578498

Sandia National Laboratories

Operated for the United States Department of Energy
by National Technology and Engineering Solutions
of Sandia, LLC.

Albuquerque, New Mexico 87185-0101
Livermore, California 94551-0969

date: November 8, 2022

to: SNL WIPP[1] Records Center
Sandia National Laboratories
4100 National Parks Highway, Building A, Carlsbad, New Mexico 88220, U.S.A.

From : Isaac Foli (idfoli@sandia.gov), Kevins Rhino, Jay Jang
Sandia National Laboratories
4100 National Parks Highway, Building A, Carlsbad, New Mexico 88220, U.S.A.

subject: MgO Suspension in DI Water for Mineral Fragment Colloid Analysis

---

I. Introduction

The actinide concentration sorbed on mineral fragment colloids (MFCs) is a parameter in the modeling of potential release scenarios for WIPP intrusion after closure. The presence of stable MFCs in suspension is a determining factor for sorbed actinide concentration. Determining environmental conditions in which different MFCs form stable suspensions is foundational to supporting the Compliance Certification Application (CCA) assumptions for modeling MFCs sorbed actinide concentrations. The WIPP inventory contains a significant mass of MgO which is used as the primary engineered barrier to restrict actinide mobility. Demonstrating the range of environmental conditions such as ionic strength (I) and acidity (pH) in which MgO forms stable MFCs suspensions is an avenue to confirm CCA assumptions and assuage Environmental Protection Agency (EPA) questions concerning the possible relationship between MgO inventory and MFCs actinide mobility.

I.1. Scope of this Memo

This memo describes initial experimentation focused on characterizing the formation and stability of magnesium MFCs from the engineered barrier MgO and is intended as the foundational groundwork

[1] SNL WIPP: Sandia National Laboratories at the Waste Isolation Pilot Plant (WIPP). WIPP is located ~26 miles southeast of Carlsbad, New Mexico, U.S.A., built 2,150 feet underground in the Salado Formation, a thick Permian evaporite deposit in the northern Delaware Basin.

WIPP:4.4.2.2.1:TD:QA-L:RELEAT 564707

Information Only

from which to assess the changing stability of MgO MFC suspensions in an increasingly complex chemical system.

Method development for the formation and stability of Mg-based MFCs is in progress. This memo reports the interim results for initial method development as a data-driven guide for future experiments. The experimental activities related to the measurements reported in this memo can be located in WIPP-Colloids-4 pages 1-24 and WIPP-Colloids-4 Binder-1.

The data presented in this memo reflect R&D work aimed at method development for future colloidal investigations. Therefore, data summarized in this memo will serve as basic analytical tools for future experiments to be performed under conditions close(r) to WIPP-relevant conditions. The data presented in this memo shall not be used to support any compliance decision.

II. Chemical System

This experiment used the non-pure MgO(s)[2], denoted MM MgO. The MM MgO was obtained from WIPP (NWP)[3] on 2022/02/17 (WIPP-Colloids-4 page 3) and was inundated with DI water. The three system components are Mg^{+2}, H^{+}, and H_2O. Effects of the impurities in the MM MgO on particle stability are not considered and remain an unquantified source of uncertainty.

III. Goals and Hypotheses

The goal is to measure the time-dependent change of the colloidal stability of suspension made of MM MgO and DI water using multiple analytical techniques. Selected analytical techniques are dynamic light scattering (DLS), laser diffraction particle size analysis (LD-PSA), scanning electron microscopy (SEM), x-ray diffraction (XRD), energy dispersive x-ray spectroscopy (EDS), pH meter and electrode, and inductively coupled plasma atomic emission spectroscopy (ICP-AES).

To partly achieve the goal above, a single reactor was prepared, which had a lifetime of 34 hours. Reactor preparation and sampling schedule are described in Section IV. Data was generated from sampling during the experiment using analytical instruments mentioned above.

[2] Mineralogical name of MgO(s): Periclase. (s) is the designator for solid phase.
[3] Nuclear Waste Partnership

Information Only

The hypothesis to be proved or rejected using the measurements is:

MFCs derived from the MM MgO will form stable colloidal particle suspensions in DI water.

IV. Reactor Preparation and Sampling

Measurements are presented in Sections V and VI. Observations are discussed in Section VII on page 23. Setup, measurement activities and data generated from this experiment are documented in Scientific Notebook WIPP-Colloids-4 pages 1-24 and its associated Scientific Notebook supplement WIPP-Colloids-4 Binder-1.

The MgO reactor (titled MgO-DI-Low-SS) was created by weighing out and adding 80.0006 g of Martin Marietta MgO (hereafter referred to as MM MgO) into a clean 1-liter HDPE bottle fitted with a length scale. After MgO addition, 720.0001 g of DI water was measured incrementally then mixed into the 1-liter HDPE bottle containing the MM MgO. The pH of the water was measured before mixing and the pH of the reactor was measured immediately after mixing. The reactor was placed onto a platform shaker and allowed to shake gently for 24 hours at 100 revolutions per minute before sampling began. All pH measurements are summarized in Table V-1 on page 6.

Following the cessation of shaking the reactor was not moved or disturbed except through minor interaction with the insertion of a pH probe and insertion of a 10 mL pipette ½" into the supernatant liquid level from which sample aliquots were drawn. Between sampling steps, the cap of the bottle was placed loosely atop the reactor. pH of the reactor was measured, and length scale recorded immediately following the cessation of shaking (0 hours) and at each subsequent sampling timestep. The reactor length scale was recorded and then measured for pH and sampled at 0, 1, 2, 3, and 5 hours following shaking.

During each sampling timestep (0, 1, 2, 3, and 5 hours):

- 50 mL of supernatant was removed from the reactor in five increments using a 10-mL pipette and placed into a 50-mL conical tube.
- 20 mL was removed from the 50-mL conical tube by drawing two 10 mL aliquots which were added sequentially to a 12.5 mL syringe fitted with a 0.2 µm Pall nylon membrane filter.

Information Only

- The filter was saturated with solution by dispensing ~1 mL of the aliquot through the syringe then the remaining solution was dispensed (between 10 mL aliquots) into a separate 50 mL conical tube. Creating, two 50-mL conical tubes, one containing non-filtered supernatant, the other containing 0.2 µm-filtered supernatant.

- 1 mL was pipetted directly from the MgO-DI-Low-SS reactor into a factory new plastic cuvette which was placed in the Zetasizer for analysis.

- 5 mL of sample was removed from each 50 mL (non-filtered and filtered) conical tube and placed into separate 10-mL class A volumetric flasks then diluted to volume using 200 µL of optima grade nitric acid and DI water. The 10-mL flasks were then decanted into separate 15-mL conical tubes. These samples reflect a 2x dilution factor for both filtered and non-filtered supernatant.

Analytical samples generated from this sampling procedure are summarized in Table IV-1 on page 4. After the final sampling time-step, the reactor was decanted into a filtration cup fitted with a Whatman grade 3 (6 µm pore) filter paper upon which a vacuum was being induced. The decanted solids were vacuum filtered for 30 minutes to minimize the water trapped in the intergranular spaces, after which the vacuum force was suspended, and a small portion of sample was removed for solid phase analysis. The vacuum filtered solids were covered and left to air dry for three days. After the air drying an additional solid phase sample was prepared. A round peg mount with carbon sticky tape was depressed into the filtered, air-dried solids and lightly agitated to remove loose particles. This peg mount was used SEM imaging and energy-dispersive spectroscopic analysis.

Table IV-1. Analytical samples generated from the sampling procedure in Section IV. Subsequent instrument analyses of samples from this table truncated the "MgO-Low-SS-DI" from the beginning of the sample name and are only identified by their timestep and filtration status (when applicable) for each instrument analysis. N denotes filtered, NF denotes non-filtered.

Sample Name	Container Type	Intended Analytical Use	Dilution Factor	Volume at time of sampling completion (mL)
MgO-Low-SS-DI-0NF	50 mL conical vial	Mastersizer 3000	1x	30
MgO-Low-SS-DI-0F	50 mL conical vial	TOC	1x	20
MgO-Low-SS-DI-0-hr	Plastic cuvette	Zetasizer	1x	1
MgO-Low-SS-DI-0NF-Mg	15 mL conical vial	ICP-AES	2x	10
MgO-Low-SS-DI-0F-Mg	15 mL conical vial	ICP-AES	2x	10

Information Only

Sample Name	Container Type	Intended Analytical Use	Dilution Factor	Volume at time of sampling completion (mL)
MgO-Low-SS-DI-1NF	50 mL conical vial	Mastersizer 3000	1x	30
MgO-Low-SS-DI-1F	50 mL conical vial	TOC	1x	20
MgO-Low-SS-DI-1-hr	Plastic cuvette	Zetasizer	1x	1
MgO-Low-SS-DI-1NF-Mg	15 mL conical vial	ICP-AES	2x	10
MgO-Low-SS-DI-1F-Mg	15 mL conical vial	ICP-AES	2x	10
MgO-Low-SS-DI-2NF	50 mL conical vial	Mastersizer 3000	1x	30
MgO-Low-SS-DI-2F	50 mL conical vial	TOC	1x	20
MgO-Low-SS-DI-2-hr	Plastic cuvette	Zetasizer	1x	1
MgO-Low-SS-DI-2NF-Mg	15 mL conical vial	ICP-AES	2x	10
MgO-Low-SS-DI-2F-Mg	15 mL conical vial	ICP-AES	2x	10
MgO-Low-SS-DI-3NF	50 mL conical vial	Mastersizer 3000	1x	30
MgO-Low-SS-DI-3F	50 mL conical vial	TOC	1x	20
MgO-Low-SS-DI-3-hr	Plastic cuvette	Zetasizer	1x	1
MgO-Low-SS-DI-3NF-Mg	15 mL conical vial	ICP-AES	2x	10
MgO-Low-SS-DI-3F-Mg	15 mL conical vial	ICP-AES	2x	10
MgO-Low-SS-DI-5NF	50 mL conical vial	Mastersizer 3000	1x	30
MgO-Low-SS-DI-5F	50 mL conical vial	TOC	1x	20
MgO-Low-SS-DI-5-hr	Plastic cuvette	Zetasizer	1x	1
MgO-Low-SS-DI-5NF-Mg	15 mL conical vial	ICP-AES	1x	10
MgO-Low-SS-DI-5F-Mg	15 mL conical vial	ICP-AES	2x	10

V. Data - Aqueous

V.1. pH

The pH of the water was measured before mixing and the pH of the reactor was measured immediately after mixing (Table V-1). After mixing, the pH was stable. The average is 11.0, and the observed scatter is confined within 2SD = 0.34 pH unit (Figure V-1). Observations are discussed in Section VII.1 on page 23.

Information Only

Table V-1. Reactor pH and length (liquid level) per sampling time-step.

Timestep	pH	Length (cm)	Date/Time
DI water	6.85	Not applicable	5/4/22 &:35 AM
Pre-Shaking	10.94	12.75	5/4/22 7:46 AM
1-hour	11.00	10.6	5/5/22 9:00 AM
2-hour	11.03	9.5	5/5/22 10:00 AM
3-hour	11.41	8.4	5/5/22 11:00 AM
5-hour	11.12	7.3	5/5/22 1:00 PM

Figure V-1. Plot of pH measurements in Table V-1. Black square at 4 hours is the average of the pH measurements with 2SD as the red error bar.

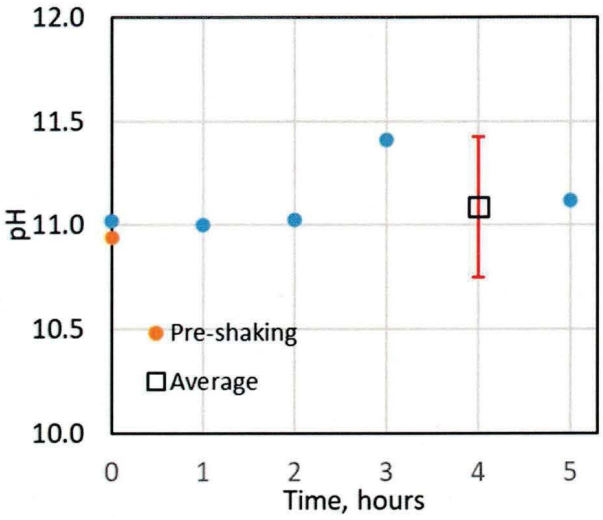

V.2. [Mg]

Atomic emission spectroscopic data of the concentration of magnesium (denoted [Mg] hereafter) in the supernatant were collected using ICP-AES over experimental lifetime. Samples for the measurements of [Mg] on ICP-AES, i.e., [Mg]ICPAES in Equation (A), were taken from the non-filtered and filtered supernatants at each timed investigation (MgO-Low-SS-DI-xNF-Mg and MgO-Low-SS-DI-xF-Mg, x = 0, 1, 2, 3, and 5; Table IV 1). The non-filtered and filtered supernatants were collected from the uppermost part of the liquid supernatant assumed to contain both colloidal and dissolved magnesium.

$$[Mg]ICPAES = [Mg]diss + [Mg]coll \text{ , and } [Mg]coll \approx \text{zero for filtered sample} \quad (A)$$

Information Only

where [Mg]ICPAES is the concentration of Mg reported by the ICP-AES, [Mg]diss is the contribution of dissolved Mg, and [Mg]coll is the contribution of Mg in the suspended colloidal Mg.

The measurements of [Mg]ICPAES for non-filtered and filtered samples were driven by the following hypotheses.

H-1: [Mg]ICPAES of the non-filtered samples would contain a component of non-zero [Mg]coll and thus would be greater than [Mg]ICPAES of filtered samples. Since [Mg]coll of filtered samples would be closer to zero as particles with size dimensions greater than the pore size of the filter are physically excluded and colloidal sized particles are excluded via electrostatic forces.

H-2: [Mg]ICPAES/Non-filtered and [Mg]ICPAES/Filtered would become identical at the later stage of investigations as colloidal particles aggregate and fall out of solution and away from the sampling horizon in the supernatant.

H-3: [Mg]ICPAES/Filtered when combined with the pH measurements could be an indicator of the thermodynamic stable solid phase(s) in the experimental system, which could be different from the results of the characterization of bulk solids.

The intensities and reported concentration for the calibration curve and analytical samples is presented in Table V-2. Trends are displayed in Figure V-2. Observations are discussed in Section VII.1 on page 23.

Table V-2. Raw ICP-AES data. Trends are displayed in Figure V-2. Grey cells represent calibration samples. Analytical samples described as #-NF/F - the number refers to the sampling timestep and the NF/F refers to the status as non-filtered or filtered. Reported concentration is restored to reflect undiluted concentration. Raw data documented in WIPP-Colloids-4 Binder-1.

Sample ID	Loaded/Reported Concentration (ppm Mg)	SD Concentration	RSD Concentration	Mean Corrected Intensity	SD Corrected Intensity
0.5 ppm	0.5	N/a	N/a	107157	5783.6
1 ppm	1.0	N/a	N/a	194848	2063.8
2.5 ppm	2.5	N/a	N/a	608288	447.2
5 ppm	5	N/a	N/a	1100794	4512.3
10 ppm	10	N/a	N/a	2460098	28886.1
Blank	0.026	0.051	194.501	-787	10714.0
1 ppm Check	0.089	0.011	1.294	194061	2488.9
0 NF	0.72	0.00	1.326	80310	1008.7
0 F	0.49	0.02	8.188	56918	4293.8
1 NF	0.76	0.01	5.085	84749	4097.4
1 F	0.61	0.00	2.549	68824	1642.7
2 NF	0.56	0.00	1.524	63323	897.5
2 F	0.49	0.01	5.789	56570	3015.1
3 NF	0.81	0.02	6.677	89647	5711.3

Information Only

Sample ID	Loaded/Reported Concentration (ppm Mg)	SD Concentration	RSD Concentration	Mean Corrected Intensity	SD Corrected Intensity
3 F	0.68	0.04	11.858	76839	8600.3
5 NF	0.93	0.09	19.559	102525	19300.6
5 F	0.24	0.01	15.110	30037	3833.6
Blank	-0.16	0.00	3.561	-12571	614.7
5 ppm Check	4.84	0.00	0.182	1099220	2145.3

Figure V-2. Scatterplot of concentration vs. timestep for Filtered and Non-Filtered ICP-AES samples. Solid lines plotted by regression of Filtered and Non-Filtered datapoints. Filtered samples in blue. Non-filtered samples in red.

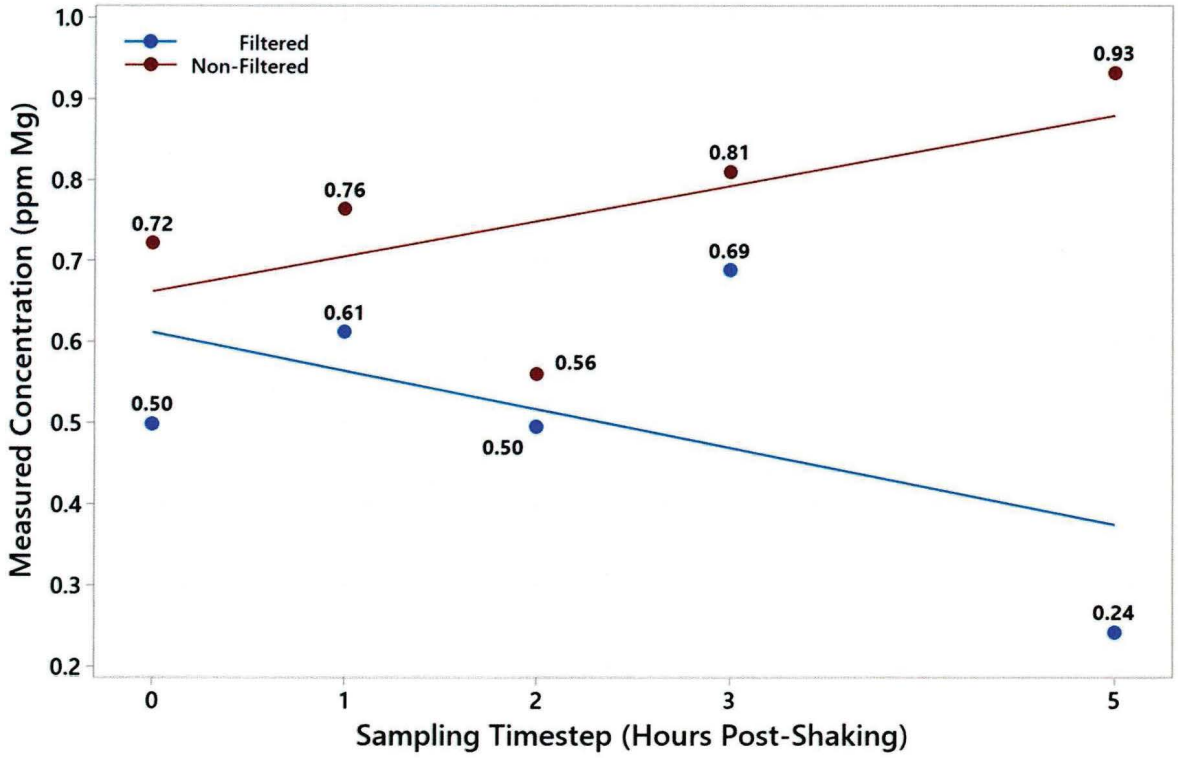

Information Only

Figure V-3. Averages of $[Mg]_{ICPAES/Non-filtered}$ and $[Mg]_{ICPAES/Filtered}$. Error bars are the 2SD of the measurements in Table V-2 and Figure V-2. Small population size of the two treatments means that more information is needed to determine statistical difference.

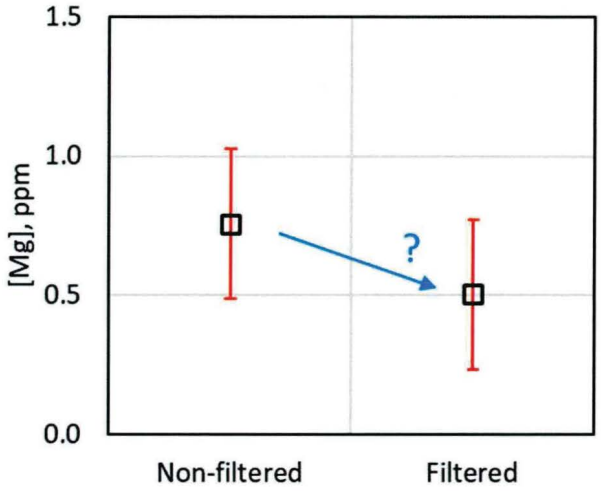

V.3. TOC

An accessory to the experimental goal was to collect data for the total dissolved concentrations of organic and inorganic carbon in the DI water and the reactor at experimental termination. The assumed sources of carbon are the atmospheric $CO_2(g)$, organic residue in the DI water, and leaching of the bottle material (HDPE). These data can be used to assess the diffusion of CO_2 into a reactor over experimental lifetime and this capability may be useful in calculating the potential saturation of carbonate mineral phases in solution in future experiments. Additionally, the data can be used to investigate the "cleanliness" laboratory DI water (in ppm of organic and inorganic carbon) and the sensitivity of the implanted workflows for our Total Organic Carbon Analyzer at SNL WIPP Geochemistry. Raw data for total carbon (TC), inorganic carbon (IC) and non-purgeable organic carbon (NPOC) are presented in Table V-3 for analytical samples and Table V-4 for DI water blank measurements. The relationship between TC, IC, and NPOC is displayed in equation B. Calibration information on the measurements of IC, TC, and NPOC is provided in Section XI on page 32.

$$TC = \text{organic carbon} + \text{inorganic carbon} \quad (B)$$

NPOC analysis includes an extra acidification and sparging step to remove CO_2 derived from inorganic components to measure only the organic carbon in the sample. Descriptive statistics for analytical and blank samples is presented in Table V-5 and trends are displayed in Figure V-4 on page 13. Observations are discussed in Section VII.2 on page 25.

Information Only

Table V-3. TOC analytical samples. Each individual sample is comprised of at least three injections which form the average concentration. Excluded (by the software) injections are inclued here and denotaed with a "1" in the "Excluded?" column. Raw data documented in WIPP-Colloids-4 Binder-1. Calibration curves displayed in Appendix XI.

Analysis Type	Sample Name	Area	Concentration	Mean Concentration	Excluded? (1 = Yes, 0 = No)
TC	TC-NF	7.67	1.12	1.22	1
TC	TC-NF	8.04	1.18	1.22	0
TC	TC-NF	8.26	1.22	1.22	0
TC	TC-NF	8.55	1.27	1.22	0
IC	IC-NF	12.14	1.68	1.70	0
IC	IC-NF	12.37	1.72	1.70	0
IC	IC-NF	12.38	1.72	1.70	0
NPOC	NPOC-NF	13.86	2.30	0.69	1
NPOC	NPOC-NF	5.89	0.92	0.69	0
NPOC	NPOC-NF	4.16	0.61	0.69	0
NPOC	NPOC-NF	3.81	0.55	0.69	0
TC	TC-NF-2	8.90	1.33	1.35	0
TC	TC-NF-2	9.06	1.35	1.35	0
TC	TC-NF-2	9.26	1.38	1.35	0
IC	IC-NF-2	13.05	1.82	1.80	0
IC	IC-NF-2	13.03	1.82	1.80	0
IC	IC-NF-2	12.72	1.77	1.80	0
NPOC	NPOC-NF-2	9.32	1.51	0.52	1
NPOC	NPOC-NF-2	4.54	0.68	0.52	0
NPOC	NPOC-NF-2	3.16	0.44	0.52	0
NPOC	NPOC-NF-2	3.17	0.44	0.52	0
TC	TC-F	10.17	1.54	1.57	0
TC	TC-F	10.29	1.56	1.57	0
TC	TC-F	10.57	1.61	1.57	0
IC	IC-F	11.33	1.56	1.57	0
IC	IC-F	11.38	1.56	1.57	0
IC	IC-F	11.49	1.58	1.57	0
NPOC	NPOC-F	12.54	2.07	0.77	1
NPOC	NPOC-F	6.11	0.95	0.77	0
NPOC	NPOC-F	4.64	0.70	0.77	0
NPOC	NPOC-F	4.39	0.66	0.77	0
TC	TC-F-2	10.58	1.61	1.64	0
TC	TC-F-2	10.87	1.66	1.64	0
TC	TC-F-2	10.83	1.65	1.64	0
IC	IC-F-2	12.56	1.75	1.65	1
IC	IC-F-2	11.81	1.63	1.65	0
IC	IC-F-2	11.98	1.66	1.65	0
IC	IC-F-2	12.04	1.67	1.65	0
NPOC	NPOC-F-2	12.59	2.08	0.66	1
NPOC	NPOC-F-2	5.42	0.83	0.66	0
NPOC	NPOC-F-2	4.41	0.66	0.66	0
NPOC	NPOC-F-2	3.44	0.49	0.66	0

Information Only

Table V-4. DI water blank TOC measurements. Excluded (by the software) injections are inclued here and denotaed with a "1" in the "Excluded?" column. Raw data documented in WIPP-Colloids-4 Binder-1. Calibration curves displayed in Appendix XI.

Analysis Type	Sample Name	Analysis Stage	Area	Concentration	Mean Concentration	Excluded? (1 = Y, 0 = No)
IC	MgO_Suspension_Blank_IC	Set-up	0.43	-0.10	-0.09	0
IC	MgO_Suspension_Blank_IC	Set-up	0.39	-0.10	-0.09	0
IC	MgO_Suspension_Blank_IC	Set-up	0.52	-0.08	-0.09	0
TC	MgO_SuspensionBlank	Set-up	0.60	0.01	0.08	1
TC	MgO_SuspensionBlank	Set-up	0.89	0.06	0.08	0
TC	MgO_SuspensionBlank	Set-up	1.06	0.09	0.08	0
TC	MgO_SuspensionBlank	Set-up	1.08	0.09	0.08	0
IC	MgO_Suspension_Blank_IC	Set-up	0.41	-0.10	-0.09	0
IC	MgO_Suspension_Blank_IC	Set-up	0.44	-0.10	-0.09	0
IC	MgO_Suspension_Blank_IC	Set-up	0.57	-0.08	-0.09	0
TC	MgO_SuspensionBlank	Set-up	0.93	0.06	0.09	1
TC	MgO_SuspensionBlank	Set-up	1.13	0.10	0.09	0
TC	MgO_SuspensionBlank	Set-up	1.05	0.08	0.09	0
TC	MgO_SuspensionBlank	Set-up	1.14	0.10	0.09	0
IC	MgO_Suspension_Blank_IC	Set-up	0.54	-0.08	-0.08	0
IC	MgO_Suspension_Blank_IC	Set-up	0.53	-0.08	-0.08	0
IC	MgO_Suspension_Blank_IC	Set-up	0.61	-0.07	-0.08	0
TC	MgO_SuspensionBlank	Set-up	0.87	0.06	0.11	1
TC	MgO_SuspensionBlank	Set-up	1.22	0.11	0.11	0
TC	MgO_SuspensionBlank	Set-up	1.25	0.12	0.11	0
TC	MgO_SuspensionBlank	Set-up	1.05	0.09	0.11	0
IC	MgO_Suspension_Blank_IC	Set-up	0.71	-0.05	-0.07	0
IC	MgO_Suspension_Blank_IC	Set-up	0.66	-0.06	-0.07	0
IC	MgO_Suspension_Blank_IC	Set-up	0.53	-0.08	-0.07	0
TC	MgO_SuspensionBlank	Set-up	1.10	0.09	0.10	0
TC	MgO_SuspensionBlank	Set-up	1.15	0.10	0.10	0
TC	MgO_SuspensionBlank	Set-up	1.23	0.12	0.10	0
NPOC	MgO_SuspensionBlank_NPOC	Set-up	0.66	0.96	0.01	1
NPOC	MgO_SuspensionBlank_NPOC	Set-up	1.10	0.96	0.08	0
NPOC	MgO_SuspensionBlank_NPOC	Set-up	0.78	0.96	0.03	0
NPOC	MgO_SuspensionBlank_NPOC	Set-up	1.00	0.96	0.07	0
NPOC	MgO_SuspensionBlank_NPOC	Set-up	0.55	0.54	-0.01	0
NPOC	MgO_SuspensionBlank_NPOC	Set-up	0.61	0.54	0.00	0
NPOC	MgO_SuspensionBlank_NPOC	Set-up	0.37	0.54	-0.04	1
NPOC	MgO_SuspensionBlank_NPOC	Set-up	0.45	0.54	-0.03	0
NPOC	MgO_SuspensionBlank_NPOC	Set-up	0.60	0.61	0.00	0
NPOC	MgO_SuspensionBlank_NPOC	Set-up	0.66	0.61	0.01	0
NPOC	MgO_SuspensionBlank_NPOC	Set-up	0.93	0.61	0.05	1
NPOC	MgO_SuspensionBlank_NPOC	Set-up	0.57	0.61	-0.01	0
NPOC	MgO_SuspensionBlank_NPOC	Set-up	0.65	0.55	0.01	0
NPOC	MgO_SuspensionBlank_NPOC	Set-up	0.40	0.55	-0.04	0
NPOC	MgO_SuspensionBlank_NPOC	Set-up	0.29	0.55	-0.06	1
NPOC	MgO_SuspensionBlank_NPOC	Set-up	0.61	0.55	0.00	0
IC	Carboy-Term-IC	Termination	0.93	-0.04	-0.04	0
IC	Carboy-Term-IC	Termination	0.85	-0.05	-0.04	0
IC	Carboy-Term-IC	Termination	0.94	-0.04	-0.04	0
NPOC	Carboy-Term-NPOC	Termination	1.19	0.10	0.04	1
NPOC	Carboy-Term-NPOC	Termination	0.81	0.03	0.04	0
NPOC	Carboy-Term-NPOC	Termination	0.90	0.05	0.04	0
NPOC	Carboy-Term-NPOC	Termination	0.77	0.03	0.04	0
IC	Carboy-Term-IC	Termination	1.03	-0.02	-0.03	0
IC	Carboy-Term-IC	Termination	0.93	-0.04	-0.03	0

Information Only

Analysis Type	Sample Name	Analysis Stage	Area	Concentration	Mean Concentration	Excluded? (1 = Y, 0 = No)
IC	Carboy-Term-IC	Termination	0.97	-0.03	-0.03	0
NPOC	Carboy-Term-NPOC	Termination	1.02	0.07	0.03	1
NPOC	Carboy-Term-NPOC	Termination	0.82	0.04	0.03	0
NPOC	Carboy-Term-NPOC	Termination	0.71	0.02	0.03	0
NPOC	Carboy-Term-NPOC	Termination	0.91	0.05	0.03	0

Table V-5. Descriptive statistics for TOC measurements presented in Table V-3 and Table V-4. Sample type is delineated in the "Sample type" column. Termination stage blank measurements reside in the grey cells.

Analysis Type	Sample type	Population (n)	Mean (ppm C)	SD (ppm C)	2 SD (ppm C)	Min (ppm C)	Max (ppm C)
IC	Analytical	12	1.68	0.09	0.18	1.56	1.82
NPOC	Analytical	12	0.66	0.17	0.34	0.44	0.95
TC	Analytical	12	1.44	0.18	0.35	1.18	0.16
IC	Blank	12	-0.08	0.02	0.03	-0.10	-0.05
NPOC	Blank	12	0.01	0.04	0.07	0.00	0.08
TC	Blank	12	0.10	0.02	0.03	0.10	0.12
IC	Blank	6	-0.04	0.01	0.02	-0.05	-0.25
NPOC	Blank	6	0.03	0.01	0.03	0.02	0.05

Information Only

Figure V-4. Individual value plot of IC and NPOC measurements by analysis stage and sample type. The left panel "A" are results from the "Setup" stage. The right panel "B" are results from the "Termination" stage including all blanks from Table V-4 analytical samples from Table V-3. Mean values for each grouping are presented in bold black numerals.

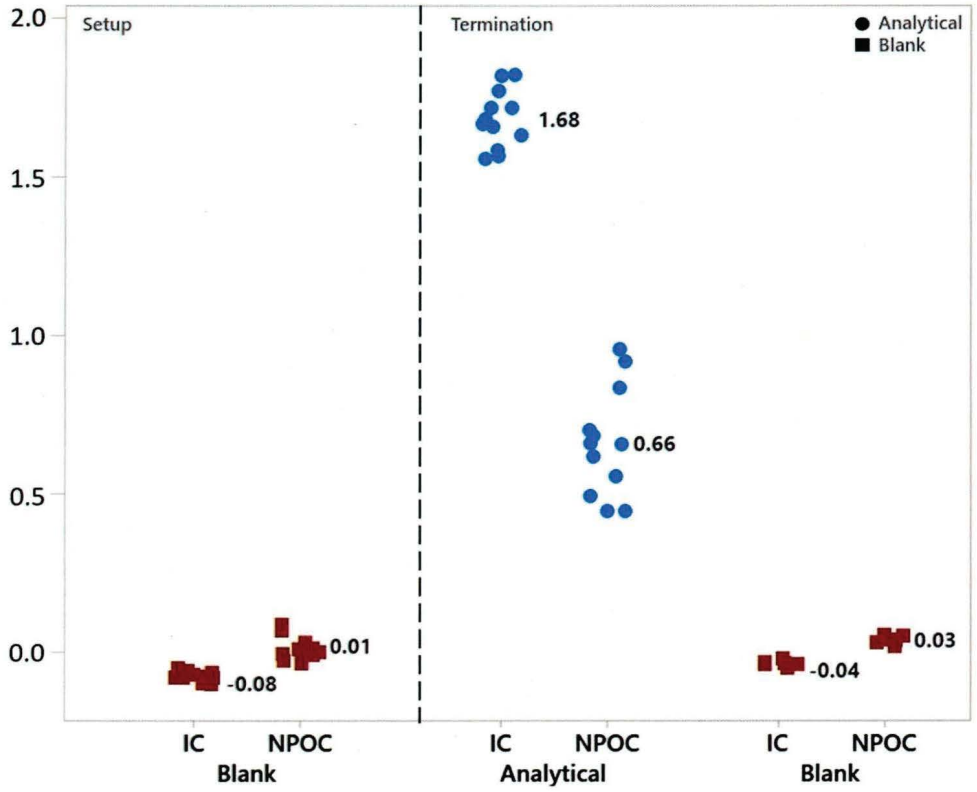

VI. Data - Colloids

This section details raw data measured for the particles and associated descriptive statistics and trends. See Sections VII.3 to VII.6 directly for observations and conclusions concerning the collected data for each analytical method.

VI.1. Zetasizer

Sample suspensions were analyzed using DLS immediately to assess the size distribution of particle size in non-filtered samples as a function of settling time. Raw data is reported including: the calculated Z-average, polydispersity index, peak 1 intensity size distribution (P1), particle concentration (where appropriate), cumulants intercept, fit error, baseline, and % in-range. Z-Average is a mean derived from the cumulants analysis conducted during measurement. The basic equation governing cumulants analysis is described in Equation (5) on page 26.

Information Only

Raw data is summarized in Table VI-1 and Table VI-2. Descriptive statistics are summarized in Table VI-3 and trends displayed in Figure VI-1 and Figure VI-2. Observations are discussed in Section VII.3 on page 25.

Table VI-1. Zetasizer size measurement data. Statistics displayed in Table VI-3. Trends displayed in Figure VI-1 and Figure VI-2. Cells marked with N/a have no report from the instrument for that parameter (i.e., particle concentration for a size measurement). MADLS measurements represent the combination of their three sub-runs (MADLS-S1/2/3). Raw data documented in WIPP-Colloids-4 Binder-1.

Sample Name	Measurement Type	Z-Average (nm)	Polydispersity Index	Particle Conc. (particles/ml)	Peak 1 Intensity size (nm)	Scatter Direction (degrees)	Intercept	Fit Error	Range (%)
0-hr_NF	Size	26200.00	0.73	N/a	N/a	174.70	1.04	0.03	84.14
0-hr_NF	Size	5986.00	1.00	N/a	35.92	174.70	0.95	0.01	67.78
1-hr_NF	Size	8156.00	1.00	N/a	N/a	174.70	1.18	0.01	64.33
1-hr_NF	Size	4411.00	1.00	N/a	169.90	174.70	0.81	0.01	52.17
2-hr_NF	Size	6479.00	1.00	N/a	39.06	174.70	1.30	0.02	78.51
2-hr_NF	Size	6430.00	1.00	N/a	9.66	174.70	1.31	0.01	69.60
3-hr_NF	Size	22200.00	0.60	N/a	N/a	174.70	1.38	0.03	85.60
3-hr_NF	Size	9071.00	1.00	N/a	N/a	174.70	1.22	0.01	70.08
5-hr_NF	Size	7550.00	1.00	N/a	8.49	174.70	1.72	0.01	90.51
5-hr_NF	Size	10000.00	1.00	N/a	N/a	174.70	1.69	0.01	80.43
5-hr_NF	MADLS	N/a	N/a	N/a	398.40	N/a	N/a	N/a	N/a
5-hr_NF	MADLS-S1	915.40	0.60	N/a	498.00	174.70	0.68	0.00	80.51
5-hr_NF	MADLS-S2	1351.00	1.00	N/a	541.40	90.00	0.70	0.01	71.90
5-hr_NF	MADLS-S3	559.20	0.74	N/a	528.60	12.78	0.77	0.01	76.87

Table VI-2. Raw Zetasizer particle concentration measurement data. Statistics displayed in Table VI-3. Trends displayed in Figure VI-1 and Figure VI-2. Cells marked with N/a have no report from the instrument for that parameter (i.e., particle concentration for a size measurement). Particle concentration measurements represent the combination of their three sub runs (P-S1/2/3). Raw data documented in WIPP-Colloids-4 Binder-1.

Sample Name	Measurement Type	Z-Average (nm)	Polydispersity Index	Particle Conc. (particles/ml)	Peak 1 Intensity size (nm)	Scatter Direction (degrees)	Intercept	Fit Error	Range (%)
0-hr_NF	Particle concentration	N/a	N/a	4.64E+06	192.90	N/a	N/a	N/a	N/a
0-hr_NF	P-S1	4214.00	1.00	N/a	260.70	174.70	0.74	0.01	50.66

Information Only

Sample Name	Measurement Type	Z-Average (nm)	Polydispersity Index	Particle Conc. (particles/ml)	Peak 1 Intensity size (nm)	Scatter Direction (degrees)	Intercept	Fit Error	Range (%)
0-hr_NF	P-S2	16300.00	0.15	N/a	N/a	90.00	0.96	0.01	50.91
0-hr_NF	P-S3	474.70	1.00	N/a	432.20	12.78	0.67	0.01	59.05
1-hr_NF	Particle concentration	N/a	N/a	7.49E+08	68.07	N/a	N/a	N/a	N/a
1-hr_NF	P-S1	3324.00	1.00	N/a	254.50	174.70	0.66	0.01	47.47
1-hr_NF	P-S2	9919.00	0.61	N/a	41.27	90.00	1.09	0.02	60.60
1-hr_NF	P-S3	13.57	1.00	N/a	717.00	12.78	0.79	0.12	85.12
2-hr_NF	Particle concentration	N/a	N/a	5.28E+08	72.89	N/a	N/a	N/a	N/a
2-hr_NF	P-S1	4274.00	1.00	N/a	108.00	174.70	1.05	0.01	62.37
2-hr_NF	P-S2	3677.00	1.00	N/a	307.50	90.00	1.08	0.01	50.09
2-hr_NF	P-S3	544.10	1.00	N/a	534.30	12.78	0.07	0.02	91.82
2-hr_NF	Particle concentration	N/a	N/a	1.43E+19	397.00	N/a	N/a	N/a	N/a
2-hr_NF	P-S1	1255.00	0.98	N/a	412.60	174.70	0.62	0.00	86.27
2-hr_NF	P-S2	936.80	1.00	N/a	576.00	90.00	0.54	0.01	76.78
2-hr_NF	P-S3	453.20	0.11	N/a	567.70	12.78	0.71	0.01	79.06
3-hr_NF	Particle concentration	N/a	N/a	4.16E+20	124.90	N/a	N/a	N/a	N/a
3-hr_NF	P-S1	9740.00	1.00	N/a	N/a	174.70	0.89	0.01	53.76
3-hr_NF	P-S2	4839.00	1.00	N/a	182.00	90.00	0.88	0.01	56.91
3-hr_NF	P-S3	742.70	1.00	N/a	676.20	12.78	0.57	0.00	57.88
3-hr_NF	Particle concentration	N/a	N/a	1.21E+21	161.40	N/a	N/a	N/a	N/a
3-hr_NF	P-S1	3377.00	1.00	N/a	217.60	174.70	0.60	0.00	72.22
3-hr_NF	P-S2	3540.00	1.00	N/a	222.50	90.00	0.81	0.01	58.86
3-hr_NF	P-S3	381.20	0.45	N/a	671.00	12.78	0.58	0.01	61.53
5-hr_NF	Particle concentration	N/a	N/a	1.05E+07	185.30	186.10	N/a	N/a	N/a
5-hr_NF	P-S1	2548.00	1.00	N/a	174.80	174.70	1.07	0.02	57.80
5-hr_NF	P-S2	3378.00	1.00	N/a	251.10	90.00	1.65	0.01	45.42
5-hr_NF	P-S3	617.40	1.00	N/a	517.90	12.78	0.62	0.00	53.98
5-hr_NF	Particle concentration	N/a	N/a	9.54E+05	379.70	N/a	N/a	N/a	N/a
5-hr_NF	P-S1	1092.00	0.63	N/a	479.30	174.70	0.73	0.01	72.68
5-hr_NF	P-S2	1579.00	1.00	N/a	371.90	90.00	0.94	0.01	55.40
5-hr_NF	P-S3	678.00	0.84	N/a	639.50	12.78	0.72	0.01	67.33

Information Only

Table VI-3. Descriptive statistics for Zetasizer raw data presented in Table VI-1 and Table VI-3. Size means, sample standard deviation (SD) and %2 standard deviations are displayed along with sample population by parameter per sampling timestep.

Parameter	Z-Average					Peak 1 Intensity Size					Parameter
Timestep	Mean (nm)	SD (nm)	2SD (nm)	%2SD	Sample population (n)	Mean (nm)	SD (nm)	2SD (nm)	%2SD	Sample population (n)	Timestep
0.00	10622.90	10483.00	14516.90	137%	5.00	242.94	164.18	328.37	143%	4	0.00
1.00	5164.71	3938.30	7876.65	153%	5.00	295.67	274.40	548.81	219%	5	1.00
2.00	3006.14	2557.00	5114.06	170%	8.00	319.35	227.46	454.92	150%	10	2.00
3.00	6740.11	7130.80	14261.62	212%	8.00	393.86	242.31	484.63	150%	7	3.00
5.00	2752.27	3150.20	6300.41	229%	11.00	401.10	181.02	362.05	95%	13	5.00

Figure VI-1. Boxplot of Z-Average particle size. Mean values (bold black numbers) are displayed alongside each timestep. All reported peak 1 intensity size values are displayed regardless of measurement type.

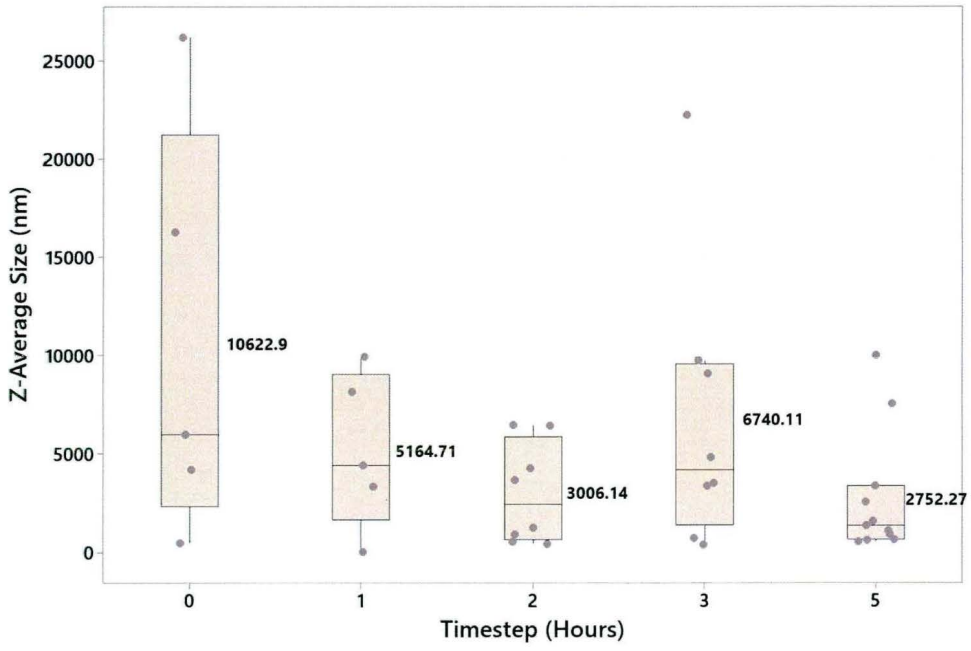

Information Only

Figure VI-2. Boxplot of P1 particle size. Mean values (bold black numbers) are displayed alongside each timestep. All reported peak 1 intensity size values are displayed regardless of measurement type.

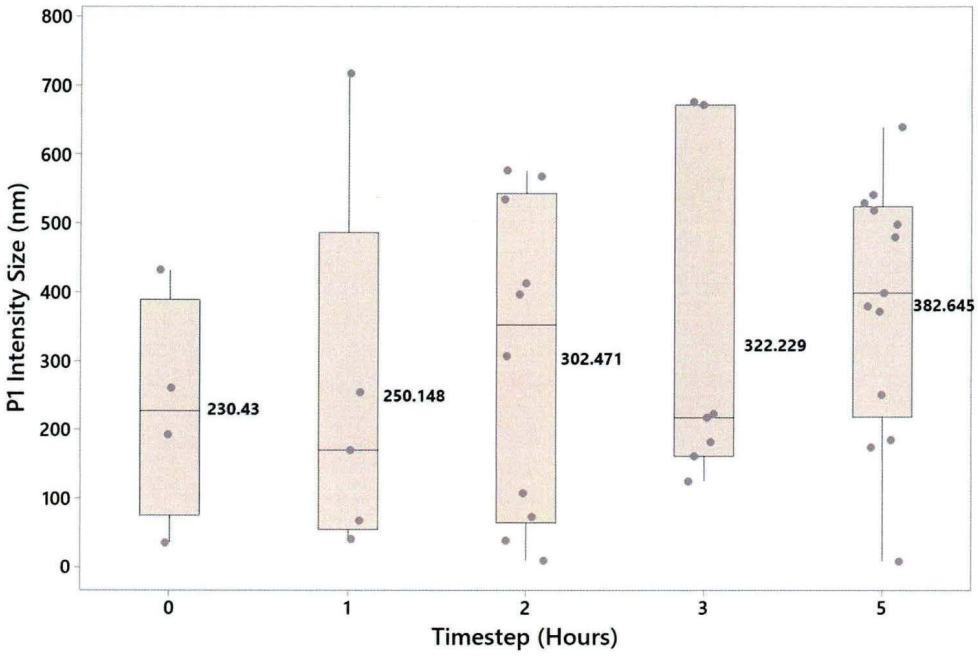

VI.2. Mastersizer

Particle size distribution data were collected via Mastersizer to assess the size distribution of suspended particles in non-filtered samples. Colloidal sized particles (operationally defined as having a size dimension less than 1 micron) may not be accurately measured by Mastersizer due to the lower manufacturer defined detection limit (0.1 μm) of the instrument. Comparing the results of Mastersizer and Zetasizer particle size distributions may help to guide experimental analysis plans moving forward.

Operational difficulties were encountered during the initial (0-hr) Mastersizer measurements. Consequently, the instrument maintenance was performed during the intervening 1- and 2-hour sampling timesteps. Additionally, the samples were not sufficiently turbid to provide optimal laser obscuration during measurement, resulting in a lower signal to noise ratio than expected during routine operation. This phenomenon is another limiting factor of the analytical technique applied to suspensions with non-optically apparent particles. Resultantly, the raw size data provided during the 0-hr timestep is unreliable although the trends presented in the 3- and 5-hour timesteps may provide some insight in context of the DLS results.

Information Only

Dara are displayed in the form Dv10,50,90. Dv refers to the X percentile of the cumulative volume distribution of particles. Thus, the mean Dv10 size would be the size below which 10% of the particles in the volume of the sample fell. Raw Mastersizer size data is presented in Table VI-4. Instrument reported descriptive statistics are summarized in Table VI-5. Data trends are displayed in Table VI-5 on page 19. Observations and conclusions are presented in Section VII.4 on page 27.

Table VI-4. Raw Mastersizer measurement data. Statistics displayed in Table VI-5 and trend displayed in Figure VI-3. Raw data documented in WIPP-Colloids-4 Binder-1

Record Number	Timestep	Dv10 (µm)	Dv50 (µm)	Dv90 (µm)
1	0-hr	1360.00	1690.00	2070.00
2	0-hr	1280.00	1710.00	2300.00
3	0-hr	833.00	1380.00	2450.00
4	0-hr	15.50	32.60	133.00
5	0-hr	1430.00	1790.00	2260.00
6	0-hr	253.00	561.00	1560.00
7	0-hr	1120.00	1740.00	2690.00
8	0-hr	1260.00	1680.00	2280.00
9	0-hr	691.00	1060.00	1750.00
10	0-hr	595.00	916.00	1480.00
11	3-hr	60.70	970.00	2150.00
12	3-hr	95.90	1100.00	2190.00
13	3-hr	43.00	257.00	423.00
14	3-hr	40.00	260.00	394.00
15	3-hr	265.00	607.00	1500.00
16	3-hr	0.79	3.33	8.96
17	3-hr	0.84	1.88	15.10
18	3-hr	0.80	1.36	7.80
19	3-hr	0.93	10.30	23.40
20	3-hr	0.72	1.04	1.45
21	3-hr	662.00	999.00	1540.00
22	3-hr	1.16	15.10	307.00
23	3-hr	10.20	87.00	793.00
24	3-hr	11.60	83.10	740.00
25	3-hr	15.80	37.60	84.60
26	3-hr	0.90	1.18	1.56
27	3-hr	0.93	1.24	1.64
28	3-hr	0.79	1.04	1.37
29	3-hr	0.80	1.07	1.41
30	3-hr	0.02	0.07	0.24
31	5-hr	207.00	357.00	613.00
32	5-hr	1070.00	1710.00	2680.00
33	5-hr	159.00	364.00	660.00
34	5-hr	1050.00	1690.00	2670.00
35	5-hr	2.39	20.10	40.90
36	5-hr	2.11	15.90	33.50
37	5-hr	1050.00	1680.00	2670.00
38	5-hr	2.03	14.60	33.10
39	5-hr	1030.00	1670.00	2660.00
40	5-hr	1.97	13.30	31.20
41	5-hr	2.00	13.30	31.40
42	5-hr	2.04	13.80	31.80
43	5-hr	1.98	13.20	29.30
44	5-hr	2.04	13.20	30.10
45	5-hr	1.93	11.70	27.30
46	5-hr	2.02	12.70	30.00

Information Only

Record Number	Timestep	Dv10 (µm)	Dv50 (µm)	Dv90 (µm)
47	5-hr	1.91	11.10	27.30
48	5-hr	2.13	11.10	25.50
49	5-hr	1.92	10.50	26.90
50	5-hr	1.87	10.00	24.90

Table VI-5. Mastersizer volume distribution percentile means calculated using the values in Table VI-4. All parameters listed in Table VI-5 are presented as reported by the instrument software. D [4,3] is the volume weighted mean. Dv(X) are the percentile at which X% of the sample is smaller than the reported size. Weighted residual is an indication of how well calculated data fits the measurment data. A good fit is indicated by a residual of under 1%.

Time Step	Mean Dv 10 (µm)	Mean Dv 50 (µm)	Mean Dv 90 (µm)	D [4, 3] (µm)	Weighted Residual
0	1360	1690	2070	1710	9.97
3	60.7	970	2150	1090	9.74%
5	207	357	613	386	34.23%

Information Only

Figure VI-3. Scatterplot of Dx (90), (50), (10) vs. measurement number. Dx (90/50/10) µm signifies 90%/50%/10% of the sample volume are below the reported particle size. Measurement duration was doubled (20x vs. 10x) for the 3- and 5-hour timesteps.

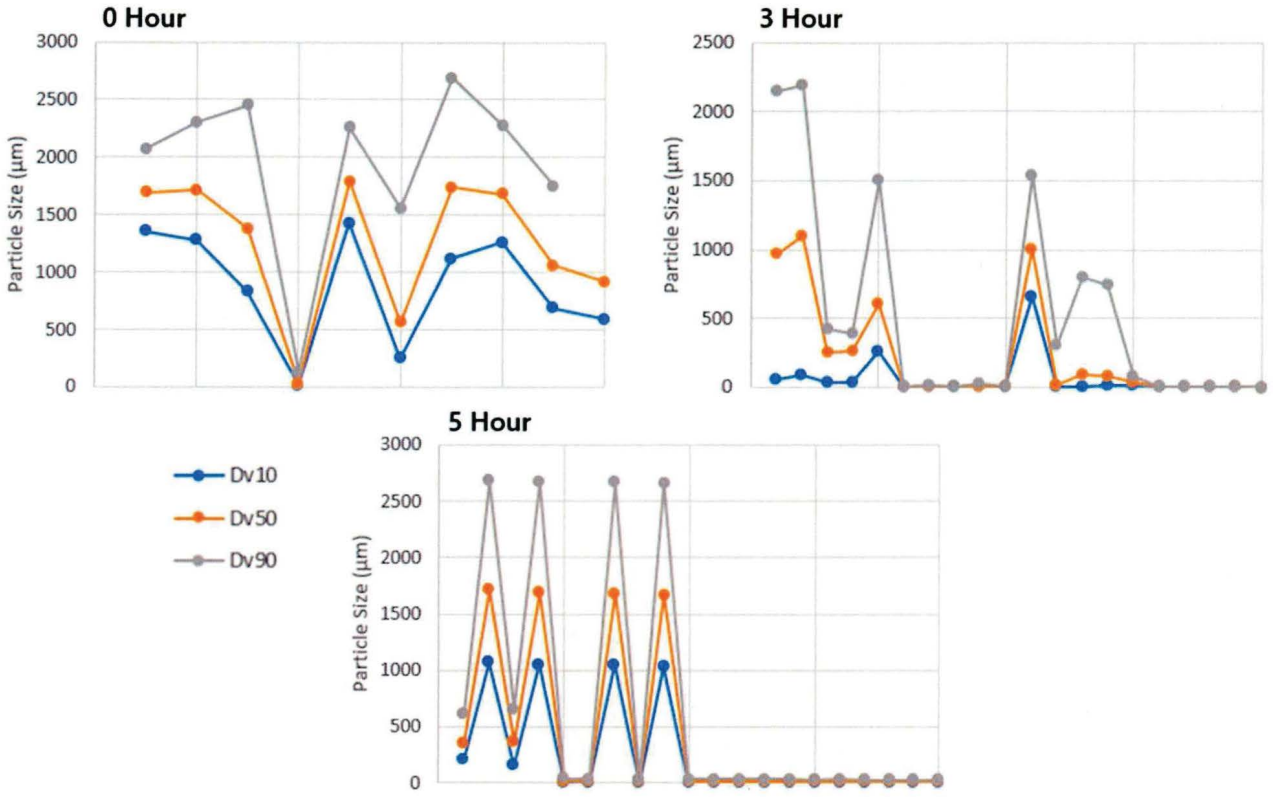

VI.3. XRD

X-ray diffraction analysis was conducted on a solid sample which was collected immediately following vacuum filtration of the solids from the reactor during termination. An additional sub-sample was analyzed after 84 hours of air-drying following termination. Diffraction patterns for periclase and brucite (PDF 00-045-0946 and 04-011-5938) are displayed alongside the sample diffraction patterns in Figure VI-4. Raw data is documented in WIPP-Colloids-4 Binder-1.

Information Only

Figure VI-4. XRD scan of vacuum filtered MgO solid from terminated reactor. Purple lines represent brucite diffraction pattern peaks. Turquoise lines represent periclase diffraction pattern peaks. Raw scan documented in WIPP-Colloids-4 Binder-1.

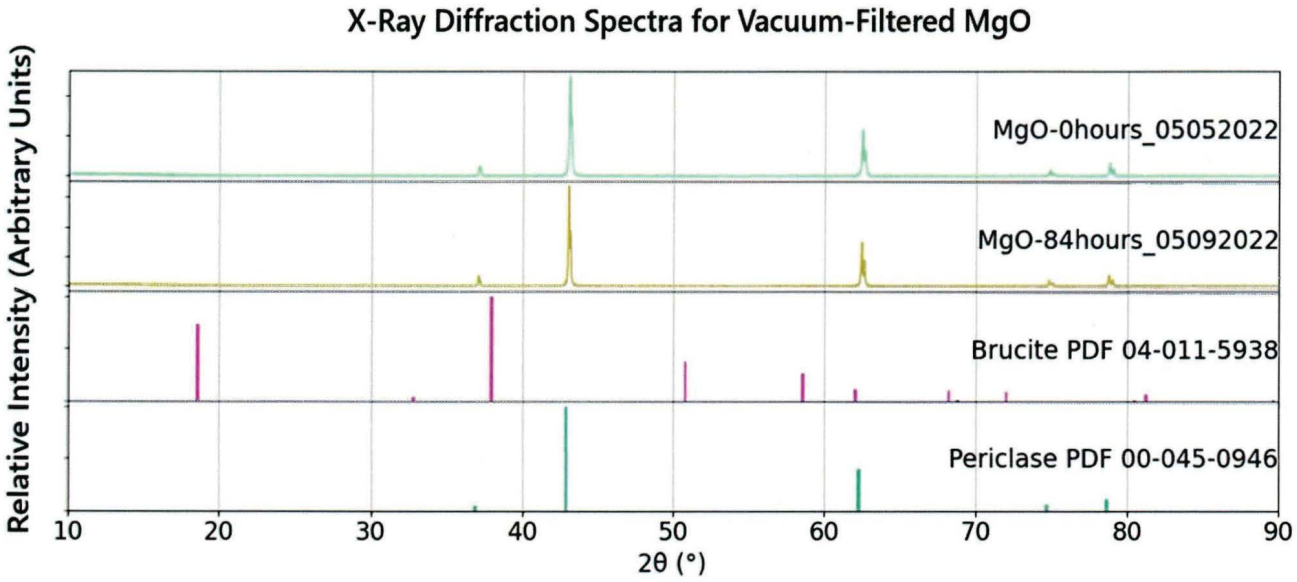

VI.4. SEM/EDS

A peg mount coated with material from the terminated reactor was loaded into the SEM and several images, and EDS scans were captured to visually assess the distribution and crystal habit of particles in the residual solid following reactor termination. A compilation of four different images at four different magnifications is presented in Figure VI-5.

Figure VI-5 exhibits that a wide distribution of sizes can be found in the primary MgO material. Particle sizes in Panel 1 reach 1 mm or more. Panel 2 exhibits agglomeration of smaller individual subhedral grains. Minor agglomeration can be observed in Panel 3 as well. Panel 4 presented the highest magnification snapshot of the sample, where subhedral rhombs exhibiting size dimensions smaller than 1 micron. Additionally, significantly smaller individual grains can be observed in the ground mass even at the highest magnification (x12,000) in Panel 4.

Information Only

Figure VI-5. SEM images of terminated and air-dried reactor material. Observable grains in the colloidal size range (less than 1 micron in one dimension) are evident. These grains do not serve to confirm the presence of colloids in the context of these images but reaffirm that possibility of observing suspended colloidal particles in subsequent experiments. Raw images documented in WIPP-Colloids-4 Binder-1.

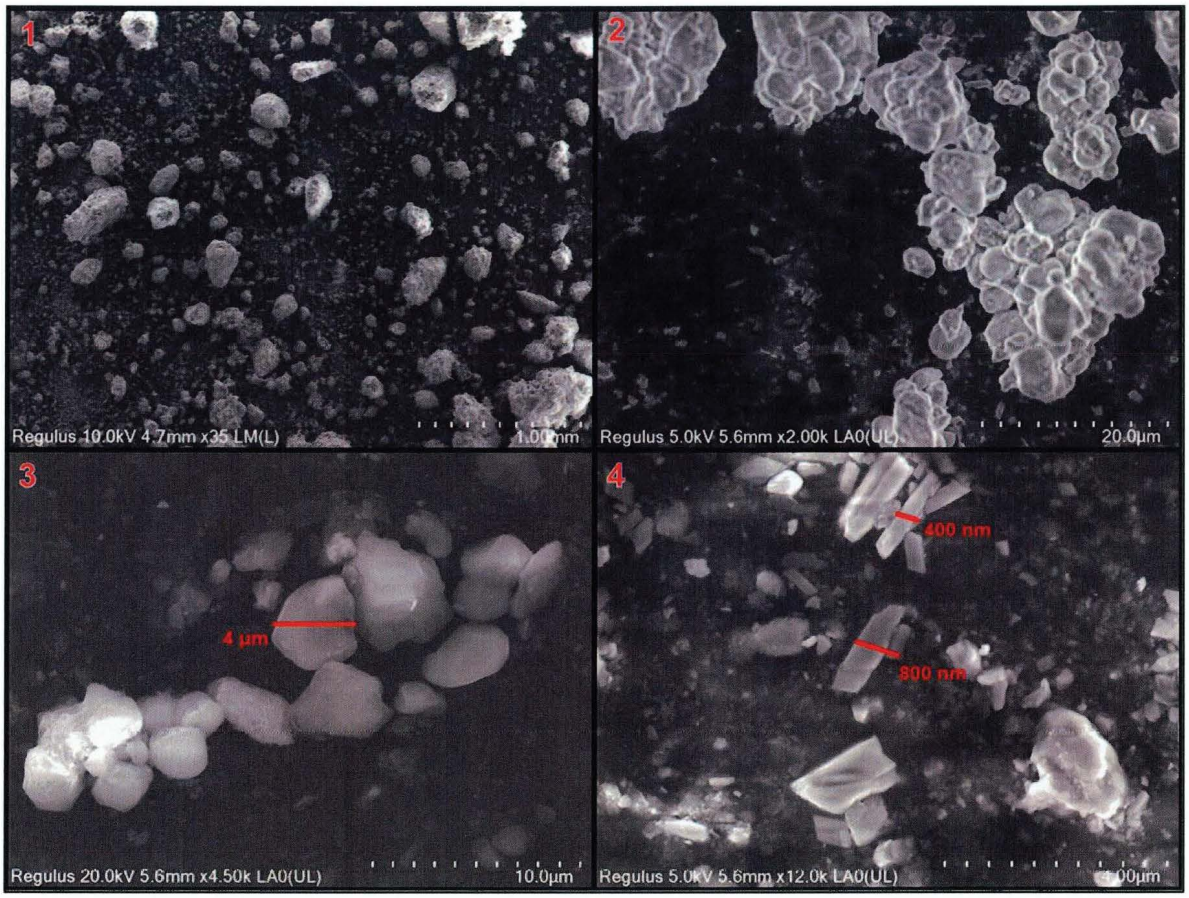

Several EDS scans were collected to assess the feasibility of EDS mapping for very small particle fractions. A single map with spectra and dominant component maps on are presented in Figure VI-6 for the same view as Panel 3 in Figure VI-5. The total counts for the spectra are very low but elemental components are still resolved with some level of clarity. Isolated compositional datapoints appear in the background away from the primary 1-5 µm particles in the center of the map.

Information Only

Figure VI-6. EDS scan of air-dried MgO solids. Panel 1 - Map. Panel 2 - Mg component map. Panel 3 - Ca component map. Panel 4 – EDS spectra. The total cps/ev is very low for the spectral map, however, the primary anticipated component of grains is resolved. Raw spectra and maps documented in WIPP-Colloids-4 Binder-1.

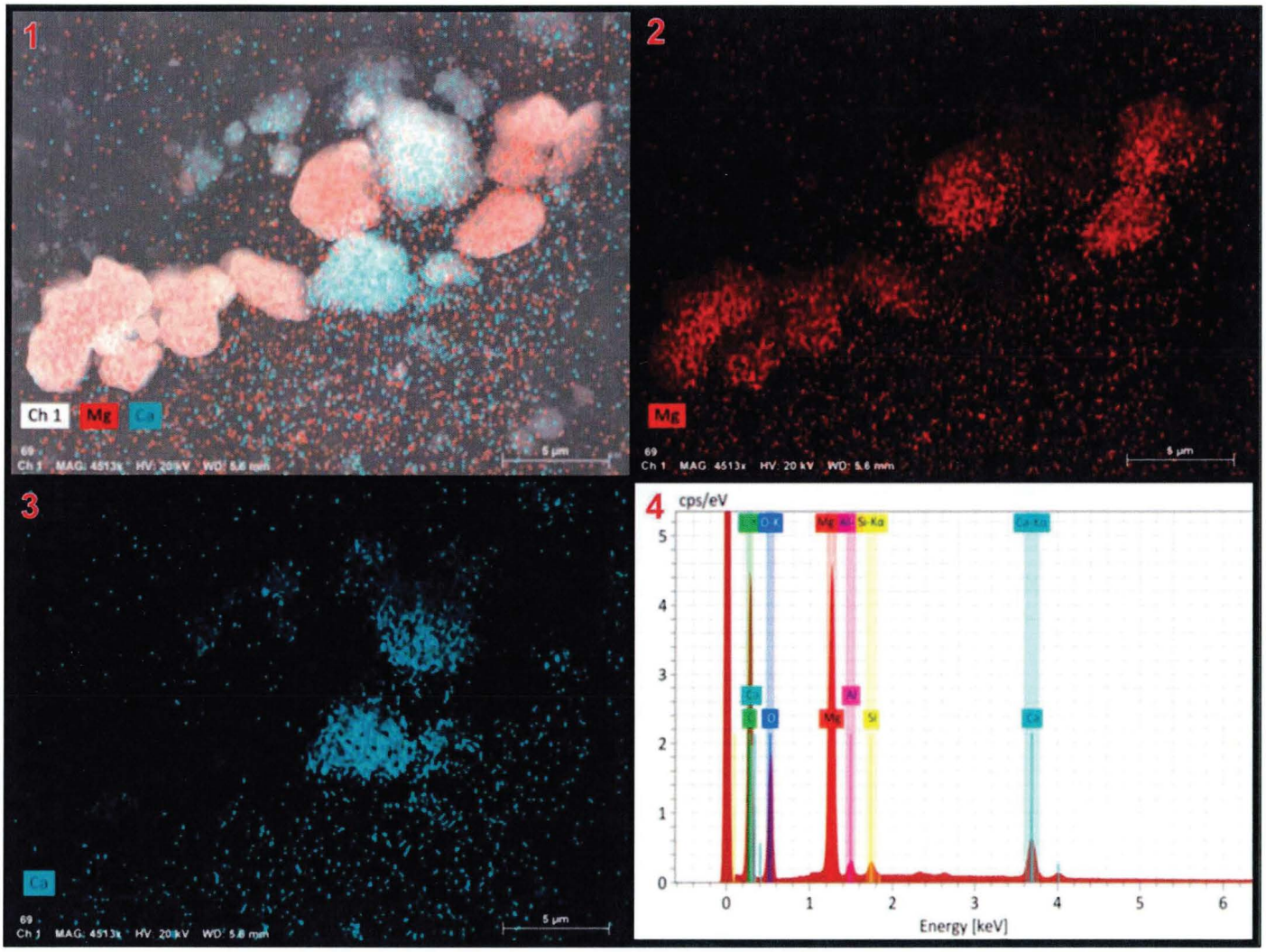

VII. Observations

Complied observations concerning raw data and trends are presented in Sections V and VI.

Subsections are discretized by analytical method before the final summary in Section IX on page 29.

VII.1. Observations – pH and [Mg]

The pH of DI water (6.85) changed to ~11 upon mixing with MM MgO. After mixing, the pH was stable for the 5-hour duration (Table V-1). The observed scatter was confined within 2SD of 0.34 pH unit (Figure V-1).

Information Only

Upon mixing of MM MgO and water the following reactions would proceed to the right:

$$MgO(s)\ (periclase) + H_2O = Mg(OH)_2(s)\ (brucite) \quad (1)$$

$$MgO(s) + 2H^+ = Mg^{+2} + H_2O \quad (2)$$

$$Mg(OH)_2(s) + 2H^+ = Mg^{+2} + 2H_2O \quad (3)$$

$$Mg^{+2} + H_2O = MgOH^+ + H^+ \quad (4)$$

where log K(1) = 4.38, log K(2) = 21.49 (Robie and Hemingway, 1973; Harvie et al., 1984), log K(3) = 17.11, and log K(4) = -11.8 (Harvie et al., 1984).

Application of the equilibrium constants above indicates that [Mg] = 218 ppm and pH = 12.0 if the MgO(s)-DI suspension is equilibrium with the initial MgO(s), or [Mg] = 3.9 ppm and pH = 10.4 if the experimental system has reached at the equilibrium with $Mg(OH)_2(s)$ due to the hydration by Reaction (1). The range of the [Mg] measurements (Figure V-2) by Average ± 2SD is 0.24 to 1.02 ppm Mg. When coupled with the pH range of 10.75 to 11.42 by Average ± 2SD (Figure V-1), the range of [Mg] indicates that both MgO(s) and $Mg(OH)_2(s)$ are undersaturated during the 29-hours of hydration. Therefore, not all the Reactions (1) to (4) are in equilibrium. Given that the aqueous reaction could be faster than the solid-state reaction (i.e., Reaction (1)), the pH seems to be buffered by Reaction (4).

While there is a consistent gap between the absolute concentration of Non-Filtered (NF) and Filtered (F) samples (~0.1 ppm; Figure V-2), the scatter of $[Mg]_{ICPAES/Non\text{-}filtered}$ and $[Mg]_{ICPAES/Filtered}$ overlap with each other (Figure V-3). Filtered samples exhibit regression with negative slope produced by a single, very low (0.242 ppm Mg relative to the next lowest reported concentration of 0.496 ppm Mg) datapoint at the final timestep as displayed in Figure V-2 on page 8. The hypotheses listed in Section V.2 cannot be tested for now because not all the Reactions (1) to (4) are in equilibrium and the wide scatters registered in the [Mg] measurements.

The inability to resolve between the two groups may be due to the closeness to the lower detection limit of the implemented ICP-AES analysis workflow. Additionally, there may be not yet understood effects from incomplete saturation of dissolved Mg species and/or colloidal size particles infiltrating the filter media. Based on these data, moving forward with experiments for determining colloidal mineral fragment presence, without concretely determining a low detection limit and ensuring the

Information Only

solubility saturation, it is not recommended to use spectroscopy as a primary investigative methodology for assessing particle suspensions, but rather only for an avenue to determine mineral phases in solution through solubility.

VII.2. Observations – TOC

Several notable trends are evident in TOC data displayed in Figure V-4 on page 13. First, mean concentrations for IC measurements are below 0. These negative mean concentrations do not reflect a real negative carbon value but represent that the IC measurements conducted on blanks produced a lower signal than the 0 point in the calibration curve used for quantification. This small (<1 ppm) difference is likely within the envelope of error for resolution with our current analytical methodology.

Second, there is not a marked increase in the concentration of IC and NPOC between the blank measurements between the set-up and termination of the experiment (Panels A and B in Figure V-4). Mean IC concentration values remain negative, and reproducibility of measurements remains high. There was not an expectation of notable $CO_{2(g)}$ intrusion into the reserved DI water of the course of the experiment. Further testing will be required to provide any useful data which may potentially supplement future studies concerning carbonation in inundated reactors.

Third, as expected the analytical samples provide a higher concentration for both IC and NPOC however IC+NPOC generally exceeds the value provided by TC measurements in Table V-3. This begs further investigation into the lower detection limit for the different operational modes on the TOC instrument (TC, IC, NPOC analysis) before meaningful conclusions are asserted for samples falling within this low (<2 ppm) range of carbon content.

VII.3. Observations - Zetasizer

The size data are broadly characterized by large Z-Average values. Z-Average is a size value calculated by the method of cumulants fitting a single exponential to the correlation function to obtain a mean size. Z-average is the result from a force fit to the initial part of the correlation function and a single exponential decay. Distribution analysis, like the intensity distributions presented in this document, fit the correlation function to longer times (Bhattacharjee 2016,). The general form of the correlation function in play for a large number of monodisperse particles in Brownian motion, $G(\tau)$, is given in Equation (5):

Information Only

$$G(\tau) = A[1 + B\exp(-2\Gamma\tau)] \quad (5)$$

Where:
τ = time
A = the baseline of the correlation function.
B = The intercept of the correlation function.
$\Gamma = Dq^2$
D = translation diffusion coefficient
$q = (4\pi n/\lambda_0)\sin(\theta/2)$
n = refractive index of the dispersant
λ_0 = wavelength of the laser
θ = scattering angle

For polydisperse samples the equation can be rewritten as is given in Equation (6):

$$G(\tau) = A[1 + B\, g_1(\tau)^2] \quad (6)$$

Where:
$g_1(\tau)$ = the sum of all exponential decays contained in the correlation function.

The Z-Average values presented in Section VI.1 (Table VI-1, Table VI-2 and Figure VI-1) are characterized by a wide distribution of values. These values reflect the effect of few, large particles or agglomerations present in the suspension at the time of measurement. This observation is supported by the polydispersity values which remain near to the maximum possible value of one for almost all samples. Additionally, reported values for intercept, fit error and % in range are indicative of an unreliable Z-Average value. The fit error describes the measure of the quality of cumulants fit to the measured data and is a general indicator of whether the Z-Average for a particular measurement is reliable. A fit error of greater than 0.005 indicates poor data quality or that a sample is too polydisperse for reliable cumulants analysis (Malvern Instruments Ltd., Malvern, UK). Fit error values for this dataset are almost uniformly greater than 0.005 lending further evidence that Z-Average values are greatly skewed by a small number (relative to the total particle count) of large particles or agglomerations.

The mean Z-Average size as displayed in Figure VI-1 by timestep exhibit an overall decreasing trend over the sampling timesteps. While mathematically these means do not exhibit a statistically significant change this negative slope is indicative of what is presumed to be occurring physically – that the large particles and agglomerations are falling out of suspension. Future work will examine the possible continuation of this trend given much longer experimental observation times.

Interestingly the converse is true of the P1 data (Figure VI-2). Size distributions are also a product of

Information Only

the correlation function but relate the scattered light intensity directly to the size without presenting a harmonic mean like Z-average. Size distribution peaks are discretized (in the case of polydisperse suspension where more than one peak is detected) based on their contribution to the total intensity of scattered light. The measured peak 1 (most prominent peak) intensity distribution particle size as displayed in Figure VI-2.

Akin to the Z-Average size means, the peak 1 sizes do not vary in a statistically significant way there is a slight positive slope in the mean values favoring increasing particle size. This trend may also be due to the settling of large and irregularity shaped particles and agglomerations trending the suspension towards a more monodisperse, stable particle suspension. While presumably that observation describes the physical reality that is occurring over the sampling lifetime it is not supported numerically by this dataset as polydispersity index remains near to maximum for the lifetime of the experiment. As stated previously, increasing experimental lifetime more than 5 hours in future experimentation, and additionally using processing models suited to measuring polydisperse suspensions during early sampling timesteps may further elucidate the relationship at play.

Overall, the Zetasizer size data exhibits a polydisperse particle suspension in which larger agglomerations and particles are continuing to fall out of suspension. Future experimentation with longer observation time will benefit from careful consideration of the application of processing models designed for polydisperse sample analysis in conjunction with alteration of scattering direction to best capture the suspension character while the suspension is evolving. Due to the presence of large settling particles and agglomerations in the solution evidenced by the high Z-averages polydispersity and poor cumulants analyses it is safe to conclude the suspension analyzed here does not reflect at any timestep a true colloidal suspension. Future experiments should significantly augment the duration of sampling and timeframe between sampling timesteps.

VII.4. Observations – Mastersizer3000

As mentioned previously in Section VI.2 on page 17, issues with the instrument arising during data collection leading to maintenance during the experiment coupled with the low laser obscuration and consequently low signal to noise ratio the numeric size results delivered by the Mastersizer are unreliable. However, observing the overall trend of measurements in the 3- and 5- hour timesteps as presented in Figure VI-3 on page 20 reveal distinct bimodality. When examined in the context of the Zetasizer results discussed in Section VII.3 the bimodal trend of Mastersizer data supports the

Information Only

conclusion that at this very young reactor settling age (hours) there are significant agglomerations or larger particles still present. Break-up of these agglomerations due to the dispersant stirring action which occurs in the Mastersizer may also lead to the very low size results delivered in the latter 10x measurements of the 3- and 5- sampling timesteps. Further testing under more optimal conditions with an experimentally ready instrument will be required to confirm these hypotheses based on initial observations.

VII.5. Observations – XRD

The X-ray diffraction spectra confirm that the MgO repository backfill material is composed dominantly of periclase (MgO(s)). Brucite ($Mg(OH)_2$(s)) is the primary reaction product expected in a purely MgO and H_2O system although whatever brucite may have formed did not do so in sufficient mass to influence the XRD results.

VII.6. Observations – SEM/EDS

SEM scans were able to identify a range of particles sizes in the terminated solids down into the operationally defined colloidal range (<1μm). Since the SEM mount was created from the terminated reactor and no from dried DLS samples these micrographs in no way represent a suspended colloidal size fraction. Further work must be undertaken to develop an analytical method for drying and mounting sampled suspensions while preventing agglomeration of particles for analysis of crystal habit, EDS analysis and/or qualitative particle characterization.

Similarly, the EDS mapping will require more work in order to dial in the best approach in order to obtain spectra with enough information to make meaningful conclusions about composition. For colloidal sized particles, collection of EDS data may prove difficult due to the nature of Mg as a light element and the X-ray interaction volume of particles with a low dimensional thickness. Proper tuning of accelerating voltage will be required to gather accurate compositional information in future analyses.

VIII. Model Parameterization

The lifetime of the sample reactor must be significantly augmented to a month or more. SNL WIPP Geochemistry believes that over such a short timeframe (<1 day) little information can be gained in context of assessing the presence or absence of colloids and/or determination of aggregation kinetics. Augmenting reactor lifetime will not only enable sufficient aggregation and sedimentation to occur

Information Only

such that a stable colloidal suspension may be achieved but also that a larger suite of time resolved measurements will enable the calculation of theoretical aggregation and settling rates if the experimental reactors never reach a steady state. Similarly, given the non-destructive and quick analysis time proffered by DLS the number of measurements executed for each sampling timestep should be augmented to enable much greater predictive statistical power for any calculations.

Accuracy of the measurements obtained from the colloid characterization techniques can be assessed by checking the equality of Equation (2) of Jang (2020), which is reproduced below (Equation (7)) for the cases where the colloidal particles are made of MgO(s) or $Mg(OH)_2$(s);

$$[Mg]_{coll} \approx \Sigma[V_p \cdot n_p]_i \times (\rho/FW) \quad (7)$$

where V_p = volume of individual particle in L, n_p = particle number density in /L, ρ = density of the particle in g/L, and FW = formula weight of the particle in g/mol. The Σ means the summation of the quantity $V_p \cdot n_p$ over cases of different particle sizes (i), which can be replaced by integration in the case of continuous distribution of particle sizes in the suspension (Jang 2020).

MgO(s) has the following properties: $\rho = 3.58$ g/cm^3 $= 3.58 \times 10^3$ g/L, FW = 40.305 g/mol. Assuming a monodisperse suspension i.e., $i = 1$, of spherical particles with diameter (d) = 4000 nm $= 4 \times 10^{-6}$ m (close to 0-hr_NF result measured under type P-S1 in Table VI-2); V_p in the right term of Equation (7) becomes $(\pi/6) \times d^3 = 0.523 \times d^3 = 33.51 \times 10^{-12}$ L. Taking n_p of 4.64×10^6 /mL $= 4.64 \times 10^9$ /mL (Table VI-2), the right term of Equation (7) becomes 13 mmol/L Mg or 315 ppm Mg.

Once SNL WIPP Geochemistry establishes the low detection limit of ICP-AES for Mg measurements, the equality of Equation (7) will be revisited using better characterization results of colloidal suspensions.

IX. Summary

The goals asserted in Section III are yet to be achieved. Based on the observations detailed above in Section VII, the view of the authors is that measurements conducted for this memo do not cover a significantly long duration of time to declare with confidence that a steady state colloidal suspension had been achieved. Or that alternatively, there is enough reliable data from that experiment such that aggregation and settling kinetics could be predicted with a high degree of confidence. Consequently, neither of the hypotheses asserted in Section III can be proved at this time. However, in so much as the experiment was a scoping study to develop our analytical approach moving forward strides have been

Information Only

made in the areas of particle detection and particle size characterization laying the groundwork for fruitful experimentation on the immediate horizon.

Particle size characterization conducted during method development for mineral fragment colloid characterization suggests that over the short duration of the experiment (<1 day) aggregation and settling of particles was still occurring. DLS analysis is sensitive to skew in the data caused by gravitationally settling or aggregating particles. The large error bars and wide spread of sizes, particularly those delivered by cumulants derived averaging techniques (Z-Average), are all indicative of sedimentation in a suspension of particles rather than a stable dispersion wherein particle movement is influenced solely by Brownian motion.

X-ray diffraction confirmed that no discernable hydration had occurred. This is consistent with the expectation for MgO(s) inundated in H_2O (Rhino et al., 2022) and the aqueous thermodynamic consideration of Section VII.1. Laser diffraction particle size analysis was confirmed to lack a low detection limit sufficient for characterization of operationally defined (<1 μm) colloidal sized particles. Laser diffraction via Mastersizer3000 will only be used in future experimentation to qualitatively assess aggregation in favor of DLS for all particle size fraction measurements. Further work needs to be conducted to determine the effectiveness of SEM and EDS for colloidal characterization. While the resolution is certainly present to image particles into the 10's of nm range, whether actionable spectra information at such a small size fraction can be achieved is yet to be seen. SEM imaging of particles in the 10-100 nm size range recovered from DLS samples during the latter steps of reactor lifetime may be useful for analysis of crystal habit in determination of hydration or other reaction products in more complicated chemical systems.

The purpose of this experiment was to aid in establishing analytical methods and dialing in techniques to be used to in-going colloid experimentation and characterization. Establishing reliable measurement approaches to characterize the stability and size of particles in aqueous suspension is the most critical facet for the success of future experiments. The data presented in this memo support the conclusion that dynamic light scattering is a tool to assess the character and evolution of a particle suspension. Despite the uncertainties and large error bars associated with the size measurements conducted during this experiment the observations gleaned not only help to inform future experimental design in terms of sampling timeframe but also analytical set-up during times of suspected particle settling and

Information Only

agglomeration. Subsequent experiments will validate whether the smaller diameter peak 1 intensity distribution sizes as seen herein represent those of a stable colloidal suspension.

Furthermore, even the augmented Z-average size values obtained by the averaging process in the DLS measurements are an order of magnitude lower than those obtained by Mastersizer analysis. While there were some noted difficulties with the Mastersizer hardware during the experiment this observation speaks to the lower detection limit of DLS, even in extremely non-ideal conditions, relative to laser diffraction particle size analysis via Mastersizer. Additionally, it has been demonstrated that DLS analysis is certainly more robust for determining the presence and possible size range of particles than utilization of the conjunction of mass spectroscopy and filtering. Several uncertainties which exist around filtering (size range band, particle – filter interaction) and the inability to differentiate between soluble and particle concentration after sample acidification can be avoided through the usage of DLS.

X-ray diffraction analysis confirm the composition of the Martin Marietta MgO received by SNL WIPP Geochemistry as essentially pure periclase (MgO(s)) although minor contaminants (calcium phase, iron phase) are present as observed in SEM and EDS analyses. Additionally, over the timeframe of the experiment conducted here no evidence of phase change due to reaction in H_2O with MgO is present. This is expected due to the very low hydration rate of MgO in water. SEM and EDS analyses confirm the presence of a wide size distribution for as-received MM MgO with large particles and agglomerations ranging from millimeter size down to nanoscale particles with size dimension less than 100 nm. Future experiments will utilize SEM with ultra-low surface roughness silicon wafer mounts to observe particles in dried colloidal suspensions. EDS is only capable of providing limited information in the particle size range presented here and will be less useful as maximum particle size decreases due to the interaction volume of the electron beam relative to particles of interest limiting collection of characteristic x-rays.

X. References

X.1. B

Bhattacharjee S. DLS and zeta potential–what they are and what they are not?. Journal of controlled release. 2016 Aug 10;235:337-51.

Information Only

X.2. J

Jang, J., 2020. Analysis Report on the Existence of Mobile Colloidal Fraction of Iron Minerals, Revision 0. GEOC-19-06. Sandia National Laboratories, Carlsbad, New Mexico, U.S.A. ERMS 572818.

X.3. R

Rhino, K., I. Foli, and J. Jang, 2022. Progress Report on the MgO Hydration and Carbonation Study at SNL WIPP Geochemistry, Revision 0. GEOC-22-10. Sandia National Laboratories, Carlsbad, New Mexico, U.S.A. ERMS PENDING as of 11/8/2022.

XI. Appendix

Figure XI-1. Set-up TC calibration curve. Samples analyzed for total carbon during the set-up step were quantified using this generated calibration curve. Set-up samples contain "suspension blank" in the sample ID

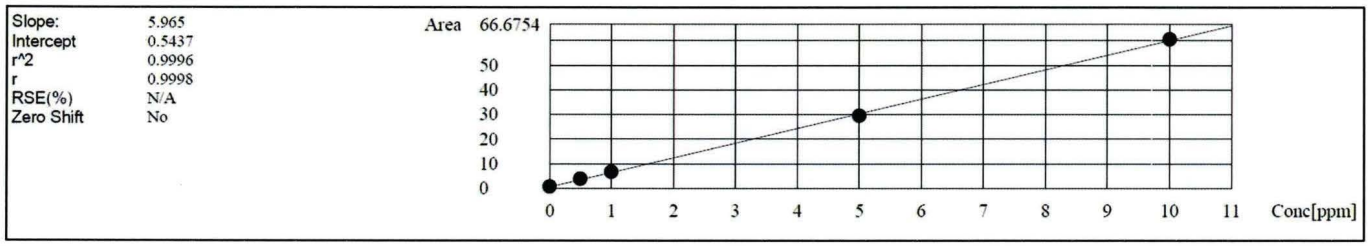

Figure XI-2. Termination TC calibration curve. Samples analyzed for total carbon during the termination step were quantified using this generated calibration curve.

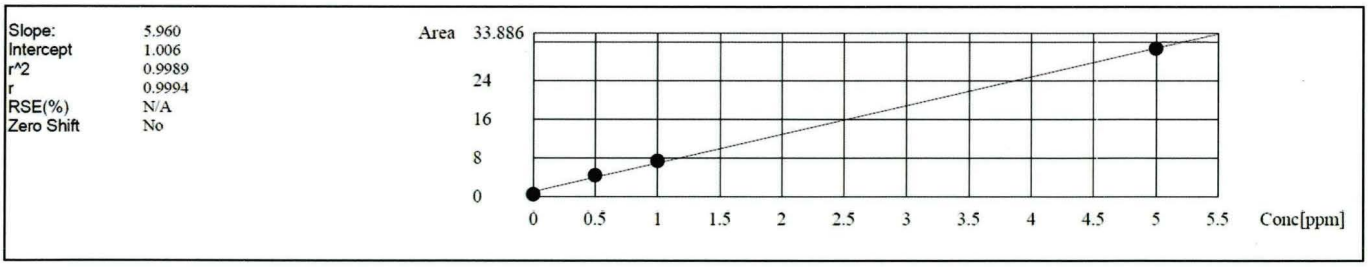

Figure XI-3. Termination IC calibration curve. Samples analyzed for inorganic carbon during the termination step were quantified using this generated calibration curve.

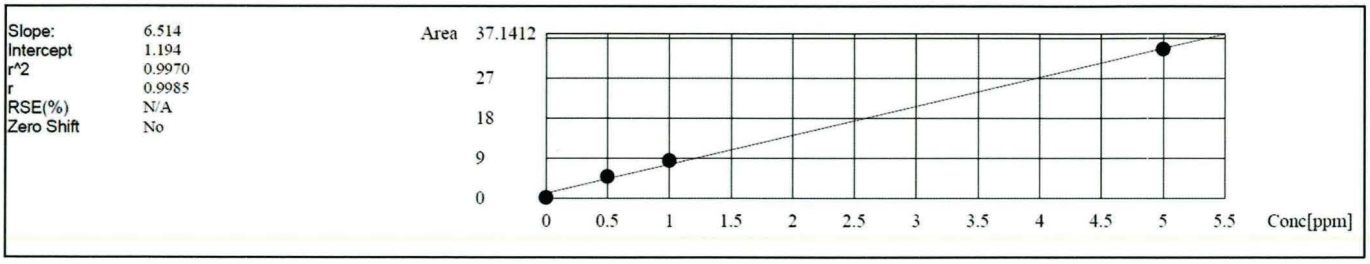

Information Only

Figure XI-4. Termination NPOC calibration curve. Samples analyzed for organic carbon during the termination step were quantified using this generated calibration curve. NPOC samples analyzed in the set-up step were also quantified using this calibration curve. Set-up samples contain “suspension blank” in the sample ID

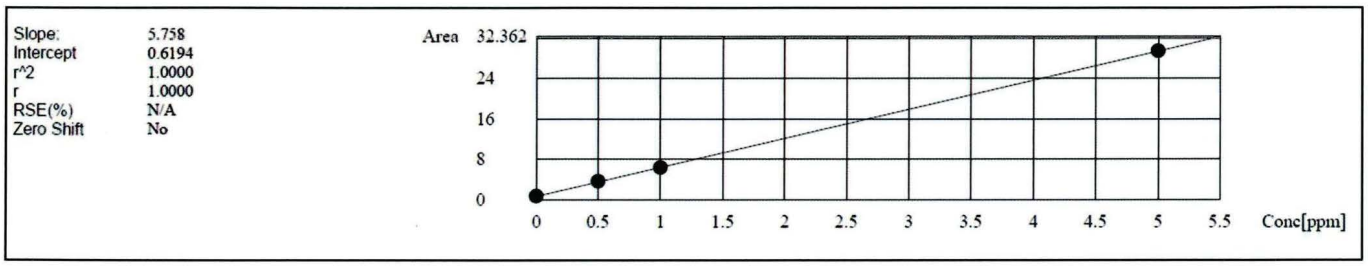

Information Only